

^{68}Ga -FAPI-04 PET Distinguishes Malignancy from Inflammatory Lesions

Chengfang Shangguan

Shanghai Jiao Tong University Medical School Affiliated Ruijin Hospital

Chen Yang

Shanghai Jiao Tong University Medical School Affiliated Ruijin Hospital

Zhaopeng Shi

Shanghai Jiao Tong University School of Medicine

Ying Miao

Shanghai Jiao Tong University Medical School Affiliated Ruijin Hospital

Wangxi Hai

Shanghai Jiao Tong University Medical School Affiliated Ruijin Hospital

Yan Shen

Shanghai Jiao Tong University Medical School Affiliated Ruijin Hospital

Qing Qu

Shanghai Jiao Tong University Medical School Affiliated Ruijin Hospital

Biao Li

Shanghai Jiao Tong University Medical School Affiliated Ruijin Hospital

Jun Mi (✉ jmei@sjtu.edu.cn)

Shanghai Jiao Tong University School of Medicine <https://orcid.org/0000-0001-5788-3965>

Research Article

Keywords: PET, fibroblast activation protein, 18F-FDG, ^{68}Ga -FAPI-04, Colitis-Associated Colorectal Cancer, AOM/DSS

Posted Date: January 5th, 2022

DOI: <https://doi.org/10.21203/rs.3.rs-1216321/v1>

License:   This work is licensed under a Creative Commons Attribution 4.0 International License.

[Read Full License](#)

Abstract

Background

The ^{68}Ga -labelled FAPI provides new oncology imaging option other than ^{18}F -FDG-PET. However, it's unclear about whether the FAPI-PET distinguishes malignancy from benign lesions.

Methods

We established an AOM/DSS-induced rat colorectal tumor model. A double PET/CT tracer of ^{68}Ga -FAPI-04 and ^{18}F -FDG was used in the rat colorectal tumor model. Histological examination, immunohistochemistry staining, and radioautography were performed in this study.

Results

^{68}Ga -FAPI PET imaging distinguishes neoplasia from inflammatory lesions in an AOM/DSS-induced rat colorectal tumor model, and FAPI accumulation gradually increases along with tumor progression. An inflammatory lesion did not interfere with ^{68}Ga -FAPI PET imaging.

Conclusion

The ^{68}Ga -FAPI-04 PET distinguishes malignant tumors from inflammatory lesions by detecting FAP in a rat colorectal tumor model, suggesting that ^{68}Ga -FAPI-04 PET is a better diagnostic tool than ^{18}F -FDG PET, at least to colorectal cancer patients.

Introduction

^{18}F -fluorodeoxyglucose (FDG) positron emission tomography/computer tomography (PET/CT) is frequently applied in cancer diagnosis and therapeutic response monitoring. However, FDG high-uptake lesions indicate carcinoma and benign lesions, such as inflammatory diseases [1, 2]. Colorectal cancer (CRC) is one of the most common malignancies worldwide. The increased uptake of FDG in the benign lesions of the colon/rectum has been described in several studies [3] [4]. Identifying malignant colorectal tumors from high FDG uptake lesions is a clinical challenge.

Fibroblast activation protein (FAP) is highly expressed in the stroma of cancer entities, including colorectal carcinomas [5–7]. A quinoline-based FAP-specific inhibitor (FAPI) was developed to target FAP as cancer-targeting molecules [8–10] and was highly promising as an imaging probe [11, 12]. In our clinical study, we have shown that ^{68}Ga -FAPI-PET provides better imaging than ^{18}F -FDG-PET.

In this study, we further evaluate the capacity of FAPI PET in distinguishing colorectal cancer diagnosis from inflammatory lesions in a rat colorectal tumor model.

Materials And Methods

AOM/DSS-induced colon cancer

Six-week-old male F344 rats were used for the AOM/DSS-induced colon cancer model. All animals were administered AOM (Sigma) by intraperitoneal injection at a 10 mg/kg dose on the first day of the first week. After one week, rats were given 2% (w/v) DSS (MP Biomedicals, Solon, OH, USA) dissolved in drinking water on the second and fourth weeks. AOM/DSS-induced colon lesions were verified by micro-enteroscopy, ^{18}F -FDG / ^{68}Ga -FAPI-04 micro-PET/CT, and pathological examination.

In Vivo PET/CT imaging on rats

AOM/DSS-induced rats were subjected to ^{18}F -FDG and ^{68}Ga -FAPI-04 micro-PET/CT analysis, performed on an Inveon MM Platform (Siemens Preclinical Solutions, Knoxville, Tennessee, USA). Rats were anesthetized with 2% isoflurane for ^{18}F -FDG (a single injection of 8-10 MBq/0.1 mL ^{18}F -FDG via tail vein) and ^{68}Ga -FAPI-04 (a single injection of 10 MBq/0.1 mL ^{68}Ga -FAPI-04 via tail vein) injection within three days. Following an uptake period of 40 mins (^{18}F -FDG) and 20 mins (^{68}Ga -FAPI-04), rats were placed on the PET scanner bed and maintained under continuous anesthesia during the study. The Inveon Acquisition Workplace (Siemens) was used for scanning. 3D regions of interest were drawn over the entire tumor guided by CT images, and tracer uptake was measured using Inveon Research Workplace software. The SUV was calculated as decay-corrected activity (kBq) per milliliter of tissue volume / injected tracer activity (^{18}F -FDG/ ^{68}Ga -FAPI-04) (kBq) per gram of body weight.

Digital autoradiography

^{68}Ga -FAPI-04 was injected via tail vein (a single injection of 10 MBq/0.1 mL) 20 min before animal euthanasia. The tumors were immediately embedded with a tissue-freezing medium (Leica, Wetzlar, Germany) and frozen after animal sacrifice. Five contiguous tissue sections of 5/10 μm thick were carried out by a 3050S cryostat microtome (Leica) for autoradiography and immunohistochemistry analysis. The tumor sections were placed in a cassette against an imaging film (Fuji, Tokyo, Japan). A Typhoon 5 (GE Healthcare, CA, USA) read the exposed plate with a Phosphor reader scanning system. The same tumor section was used for autoradiography, and the adjacent sections were used for histological assays.

Immunohistochemistry

Immunohistochemistry of FAP and HK2 was performed using the tumor sections obtained from induced rats' colorectal lesions. Slides containing the sections were stained with antibodies against HK2 (2867S,

Cell Signaling Technology) or FAP (ab207178, Abcam). After microwaving for 5 mins, 3 times, endogenous peroxidase was neutralized with 3% hydrogen peroxidase in methanol for 15 mins at room temperature, and primary antibodies were applied at 4°C overnight. Anti-rabbit IgG biotinylated secondary antibody was applied for 30 mins at 37°C, followed by SA-HRP for 30 mins at 37°C. The sections were visualized using DAB for 5 minutes and counterstained in Mayer's hematoxylin for 20 minutes.

Statistical analysis

Data were presented as mean \pm SD. The student *t*-test was used to compare two variables. A *p*-value of 0.05 or less was considered to be significant. Statistical analysis was performed using SPSS Statistics software (version 24.0.0; IBM).

Results

⁶⁸Ga-FAPI PET only reveals neoplasia in a rat colorectal tumor model

Since the AOM/DSS could spontaneously induce inflammation-associated carcinogenesis in the colorectum, we established an AOM/DSS-induced rat colorectal tumor model to test whether FAPI-PET distinguishes malignancy from benign lesions. This model perfectly represents the pathological changes of human colorectal carcinomas (CRC) from normal-aberrant crypt foci–adenoma-carcinoma. The SUVmax of ⁶⁸Ga-FAPI-04 and ¹⁸F-FDG PET were synchronously analyzed on rats administered with the AOM/DSS.

The FDG uptake increased in the colorectal region of all rats (*n*=8). The localization of the ¹⁸F-FDG was diffuse in the distant colon, proximal colon, and even intestine. In FAPI PET-positive cases, the localization of the ⁶⁸Ga-FAPI was almost always in the distant colon. The SUVmax of ¹⁸F-FDG in the colorectal region varied from 1.6 to 4.8 in the fourth month, while the SUVmax of ⁶⁸Ga-FAPI ranged from 0.3 to 4.5 (Fig. 3A). After the dissection, some of the rats were nodular hyperplasia and bowel wall invasion, and the others were only congestion and edema of the bowel (Fig. 3B).

Eight rats were divided into two groups, the neoplasia group and the inflammation group without neoplasia (Fig. 2B), which were verified by pathological examination (Fig. 3C). The expression of FAP and hexokinase2 (HK2) was detected by IHC in the neoplasia or the inflammatory tissue. HK2 is a key glycolysis enzyme. As shown in Fig. 3C, the HK2 expression was upregulated in both the inflammatory lesion and the neoplasia. In contrast, the FAP expression was increased merely in neoplasia. This observation was highly consistent with the double tracer imaging of FDG-PET and FAPI-PET (Fig. 3D). The SUVmax of ¹⁸F-FDG was 2.325 ± 0.64 and 2.250 ± 1.74 in the neoplasia group and in the inflammation group (*p* = 0.9380), while the SUVmax of ⁶⁸Ga-FAPI-04 was 3.475 ± 1.07 in the neoplasia group and 0.675 ± 0.33 in the inflammation group (*p* = 0.0024), suggesting that ⁶⁸Ga-FAPI PET imaging distinguishes malignancy from inflammation.

⁶⁸Ga-FAPI PET distinguishes malignancy from inflammatory lesions

Moreover, the ^{18}F -FDG PET and ^{68}Ga -FAPI-04 PET were performed on one rat with invasive neoplasia and polyp to avoid background interference. As shown in Fig. 3E, the invasive neoplasia was ^{18}F -FDG-positive and ^{68}Ga -FAPI-04 positive, while the polyp was only ^{18}F -FDG positive. Two lesions were located in different parts of the colorectum (Fig. 3F). Consistent with the report, the AOM/DSS-induced tumors were more often in the distal colorectum [13]. After dissection, the slices from two segments were analyzed by the autoradiography of ^{68}Ga -FAPI-04 and the FAP staining. As shown in the lower panel of Fig. 3F, the radiation intensity of the distal slice was much higher than the proximal one. Consistent with the autoradiography, only the distal sections were FAP-positive. This malignant lesion was further confirmed by pathological examination (Fig. 3G).

^{68}Ga -FAPI PET signal increases along with colorectal cancer progression

To determine whether ^{68}Ga -FAPI-04 PET can distinguish tumors from premalignant lesions, we synchronously analyzed the SUVmax of ^{68}Ga -FAPI-04 and ^{18}F -FDG PET at the indicated time points after AOM/DSS administration in a rat colorectal tumor model. After three months of administering AOM/DSS, ^{18}F -FDG and ^{68}Ga -FAPI-04 PET imaging (n=3) was synchronously performed monthly. As shown in Fig. 4A, the uptake of FDG was already high in the third month. The SUVmax of ^{18}F -FDG was 3.5 ± 0.5 at the third month, while the SUVmax of ^{68}Ga -FAPI-04 was only 0.227 ± 0.07 . However, the ^{68}Ga -FAPI-04 signal progressively increased since the third month. The SUVmax of ^{68}Ga -FAPI-04 reached 1.867 ± 0.47 in the sixth month. However, FDG SUVmax was still 4.63 ± 1.06 at the same time point (Fig. 4B). The change fold of the SUVmax of ^{68}Ga -FAPI-04 was 8.67 ± 2.68 at the sixth month compared with the third month ($p < 0.05$), while the change fold of the SUVmax of ^{18}F -FDG was 1.32 ± 0.13 . There were no significant changes in rat weight, which was 1.09 ± 0.14 (Fig. 4B). This observation further supported the above finding that non-malignant inflammation does not affect ^{68}Ga -FAPI PET imaging, distinguishing neoplasia from inflammation.

Discussion

High uptake of FDG in the intestine is nonspecific as the ^{18}F -FDG is known to accumulate in acute inflammatory lesions. Therefore, high uptake of FDG could present in various colon and rectum diseases, including tumor, polyp, Crohn's disease, or colitis [14, 15]. However, no optimal management algorithm is helpful for patients with incidental colorectal ^{18}F -FDG PET-avid lesions. Thus, it's challenging to distinguish a malignant tumor from inflammatory diseases based on the FDG uptake [3].

This study found that FAPI-04 was uptaken by the AOM/DSS-induced rat CRC tumor, where the washout was slower than the other organs except the kidney and bladder. Also, it has a high tumor-to-background contrast ratio *in vivo*. Moreover, the increased accumulation of FAPI was only in colorectal carcinomas. The ^{68}Ga -FAPI-04 signal was negative or low at the inflammatory lesions, where ^{18}F -FDG uptake was markedly increased. Therefore, the specificity of ^{68}Ga -FAPI PET is more than ^{18}F -FDG PET, at least to colorectal carcinomas.

Conclusion

This study has demonstrated that ^{68}Ga -FAPI-04 PET distinguishes malignant tumors from inflammatory lesions by detecting fibroblast activation protein (FAP) in a rat colorectal tumor model, suggesting that ^{68}Ga -FAPI-04 PET is a better diagnostic method than ^{18}F -FDG PET, at least to colorectal cancer patients.

Declarations

Ethics approval and consent to participate

This study received animal ethics board approval at Shanghai Jiao Tong University School of Medicine.

Competing interests

The authors state that no conflict of interest to disclose.

ACKNOWLEDGMENTS

We are sincerely grateful to our colleagues for their valuable suggestions and technical assistance for this study.

This study was supported by grants from the Ministry of Science and Technology of the People's Republic of China (2018YFC1313205), the Shanghai Committee of Science and Technology (11DZ2260200) (20JC1410100), and the National Natural Science Foundation of China (81572300) (81872342) to Dr. Mi, the National Natural Science Foundation of China (81801725) to Dr. Shangguan.

References

1. Divisi D, Barone M, Zaccagna G, Crisci R. Fluorine-18 fluorodeoxyglucose positron emission tomography in the management of solitary pulmonary nodule: a review. *Ann Med*. 2017,49:626-35. doi:10.1080/07853890.2017.1339906.
2. El-Galaly TC, Villa D, Gormsen LC, Baech J, Lo A, Cheah CY. FDG-PET/CT in the management of lymphomas: current status and future directions. *J Intern Med*. 2018,284:358-76. doi:10.1111/joim.12813.
3. Kousgaard SJ, Thorlacius-Ussing O. Incidental colorectal FDG uptake on PET/CT scan and lesions observed during subsequent colonoscopy: a systematic review. *Tech Coloproctol*. 2017,21:521-9. doi:10.1007/s10151-017-1652-6.
4. Kousgaard SJ, Gade M, Petersen LJ, Thorlacius-Ussing O. Incidental detection of colorectal lesions on ^{18}F -FDG-PET/CT is associated with high proportion of malignancy: A study in 549 patients. *Endoscopy International Open*. 2020,08:E1725-E31. doi:10.1055/a-1266-3308.
5. Henry LR, Lee HO, Lee JS, Klein-Szanto A, Watts P, Ross EA, et al. Clinical implications of fibroblast activation protein in patients with colon cancer. *Clin Cancer Res*. 2007,13:1736-41.

doi:10.1158/1078-0432.CCR-06-1746.

6. Guinney J, Dienstmann R, Wang X, de Reynies A, Schlicker A, Sonesson C, et al. The consensus molecular subtypes of colorectal cancer. *Nat Med*. 2015,21:1350-6. doi:10.1038/nm.3967.
7. Coto-Llerena M, Ercan C, Kancherla V, Taha-Mehlitz S, Eppenberger-Castori S, Soysal SD, et al. High Expression of FAP in Colorectal Cancer Is Associated With Angiogenesis and Immunoregulation Processes. *Front Oncol*. 2020,10:979. doi:10.3389/fonc.2020.00979.
8. Siveke JT. Fibroblast-Activating Protein: Targeting the Roots of the Tumor Microenvironment. *J Nucl Med*. 2018,59:1412-4. doi:10.2967/jnumed.118.214361.
9. Jansen K, Heirbaut L, Cheng JD, Joossens J, Ryabtsova O, Cos P, et al. Selective Inhibitors of Fibroblast Activation Protein (FAP) with a (4-Quinolinoyl)-glycyl-2-cyanopyrrolidine Scaffold. *ACS Med Chem Lett*. 2013,4:491-6. doi:10.1021/ml300410d.
10. Poplawski SE, Lai JH, Li Y, Jin Z, Liu Y, Wu W, et al. Identification of selective and potent inhibitors of fibroblast activation protein and prolyl oligopeptidase. *J Med Chem*. 2013,56:3467-77. doi:10.1021/jm400351a.
11. Loktev A, Lindner T, Mier W, Debus J, Altmann A, Jager D, et al. A Tumor-Imaging Method Targeting Cancer-Associated Fibroblasts. *J Nucl Med*. 2018,59:1423-9. doi:10.2967/jnumed.118.210435.
12. Loktev A, Lindner T, Burger E-M, Altmann A, Giesel F, Kratochwil C, et al. Development of Fibroblast Activation Protein–Targeted Radiotracers with Improved Tumor Retention. *Journal of Nuclear Medicine*. 2019,60:1421-9. doi:10.2967/jnumed.118.224469.
13. Pan Q, Lou X, Zhang J, Zhu Y, Li F, Shan Q, et al. Genomic variants in mouse model induced by azoxymethane and dextran sodium sulfate improperly mimic human colorectal cancer. *Sci Rep*. 2017,7:25. doi:10.1038/s41598-017-00057-3.
14. Prabhakar HB, Sahani DV, Fischman AJ, Mueller PR, Blake MA. Bowel hot spots at PET-CT. *Radiographics*. 2007,27:145-59. doi:10.1148/rg.271065080.
15. Kim S, Chung JK, Kim BT, Kim SJ, Jeong JM, Lee DS, et al. Relationship between Gastrointestinal F-18-fluorodeoxyglucose Accumulation and Gastrointestinal Symptoms in Whole-Body PET. *Clin Positron Imaging*. 1999,2:273-9. doi:10.1016/s1095-0397(99)00030-8.

Figures

Figure 1

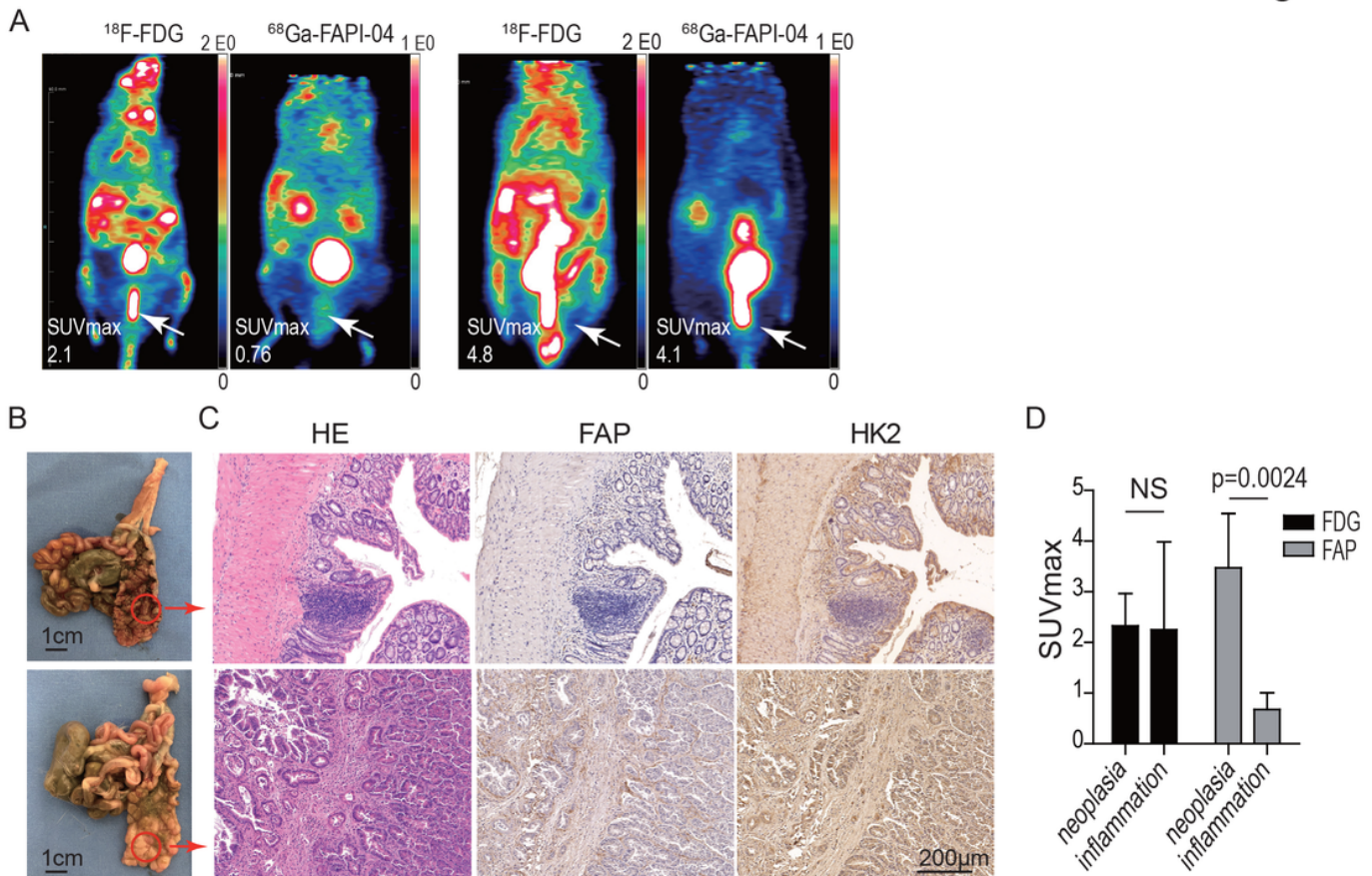


Figure 1

^{68}Ga -FAPI PET only reveals neoplasia in a rat colorectal tumor model

A. Representative images of 18F- FDG positive/68Ga-FAPI-04 negative (left) and 18F- FDG positive/68Ga-FAPI-04 positive (right) colorectal lesions (arrow).

B. Representative enteric anatomy photos: the upper (FDG +/ FAPI -) was congestion and edema of the bowel; the lower (FDG +/ FAPI +) was nodular hyperplasia and bowel wall invasion.

C. The H&E, FAP and HK2 staining in parallel sections. The Upper section was the inflammatory lesion, the lower section was the neoplasia.

D. The SUVmax of the 18F- FDG and 68Ga-FAPI-04 in the neoplasia and in the inflammatory lesions.

Figure 2

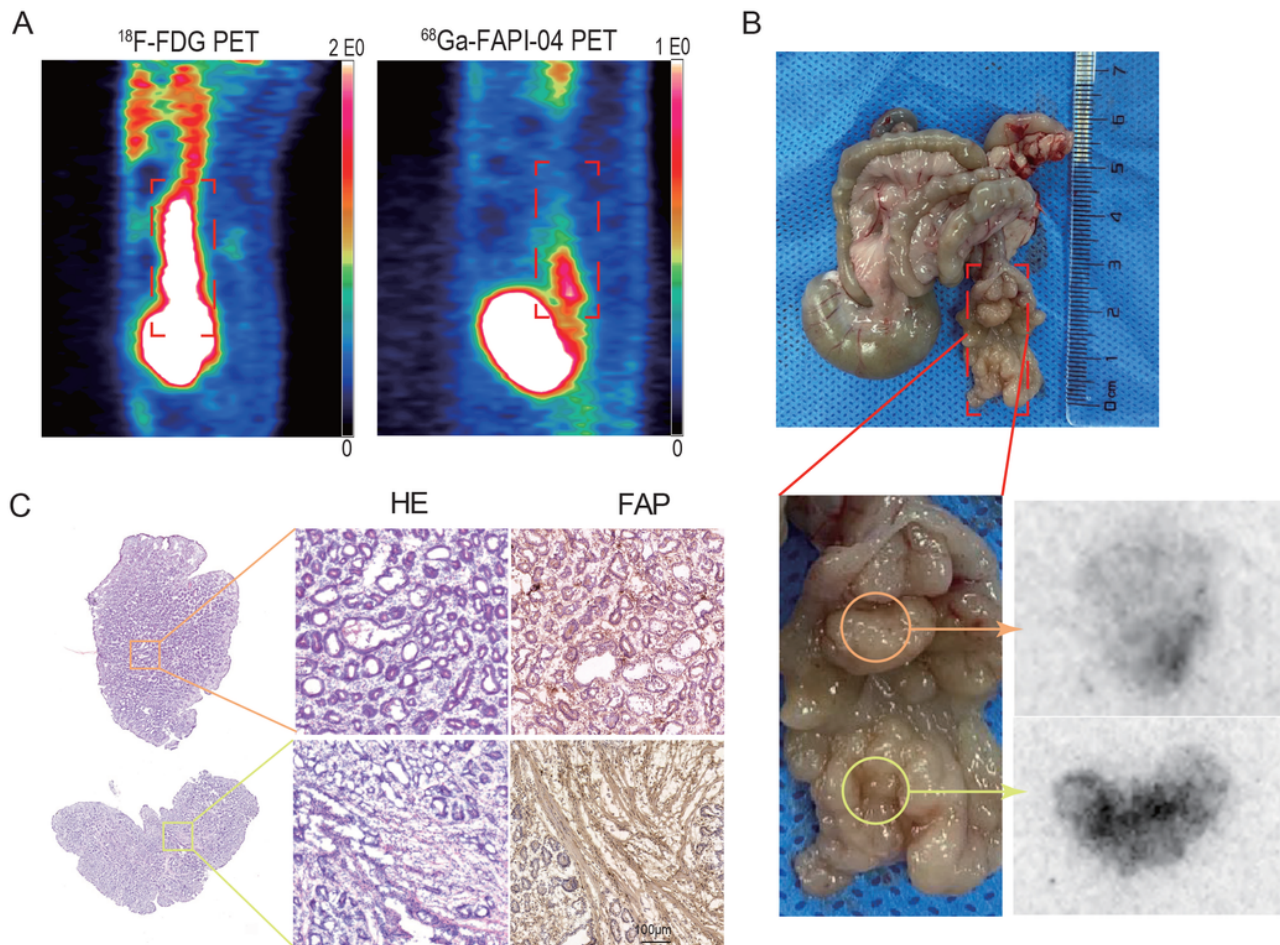


Figure 2

^{68}Ga -FAP PET distinguishes malignancy from inflammatory lesions

A. The SUVmax of ^{18}F -FDG and ^{68}Ga -FAP PET in the neoplasia and in the inflammation part of one rat.

B. Enteric anatomy photos and autoradiography images of ^{68}Ga -FAP PET. The upper was FDG +/- FAP - (orange circle), the lower was FDG +/- FAP + (yellow circle).

C. The H&E and FAP staining on the parallel sections.

Figure 3

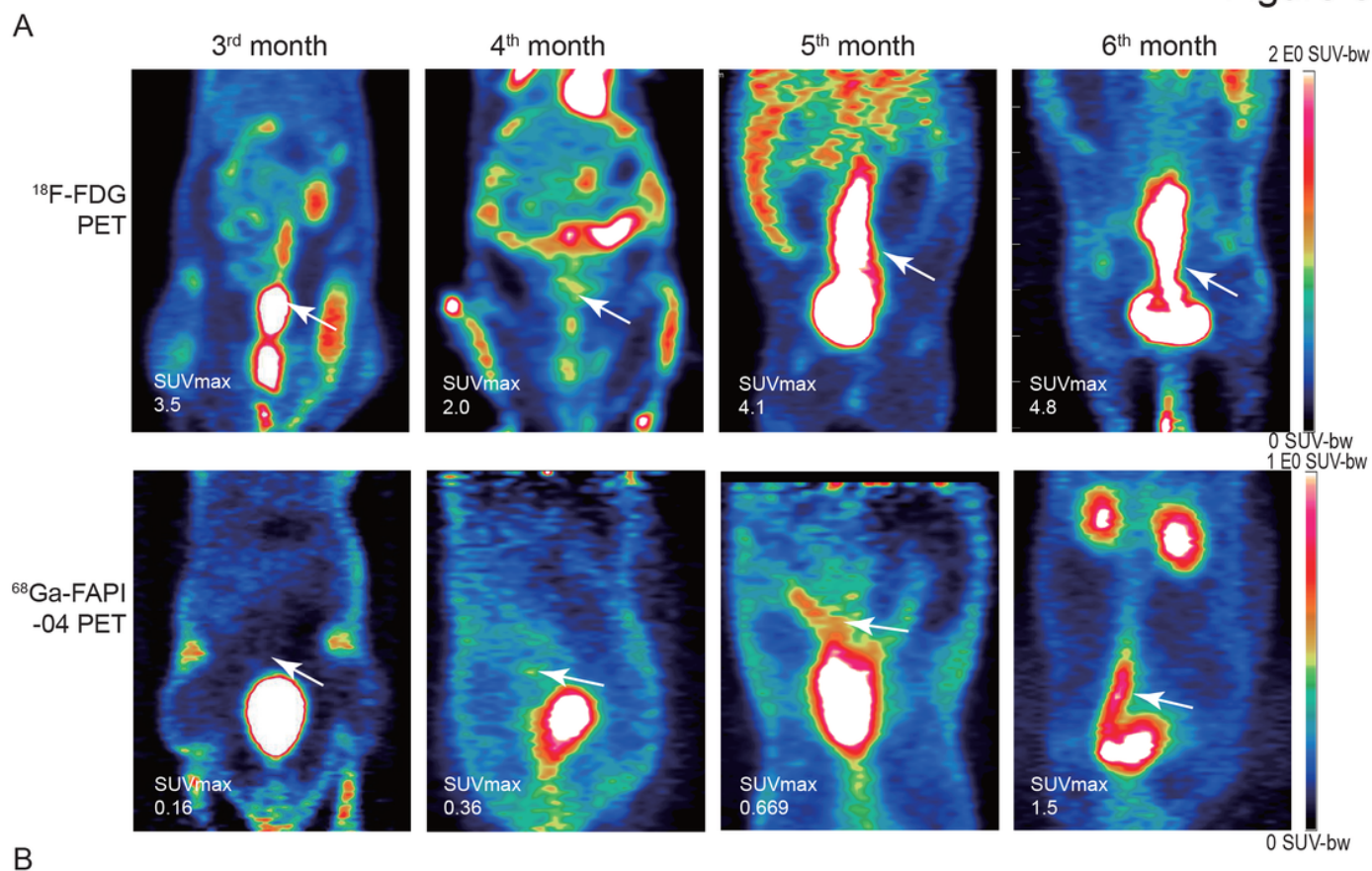


Figure 3

⁶⁸Ga-FAPI PET signal increases along with colorectal cancer progression

A. Representative images of ¹⁸F-FDG PET and ⁶⁸Ga-FAPI-04 PET in an AOM/DSS-induced rat colorectal cancer from 3rd month to 6th month.

B. Dynamic changes of ¹⁸F-FDG signals and ⁶⁸Ga-FAPI-04 signals in an AOM/DSS-induced rat colorectal tumor model. The ratios represent the change folds of the ⁶⁸Ga-FAPI-04 SUVmax, the

18F-FDG SUVmax, and the weight from the indicated time point to the 3rd month. The difference of 68Ga-FAPI-04 SUVmax between the indicated time points and the 3rd month is significant, *: $P < 0.05$.